Exact analysis of intrinsic qualitative features of phosphorelays using mathematical models

Michael Knudsen [a,b], Elisenda Feliu [c], Carsten Wiuf [c,*]

[a] Bioinformatics Research Centre, Aarhus University, Aarhus, Denmark
[b] Centre for Membrane Pumps in Cells and Disease, Aarhus University, Aarhus, Denmark
[c] Department of Mathematical Sciences, University of Copenhagen, Copenhagen, Denmark

ARTICLE INFO

ABSTRACT

Phosphorelays are a class of signaling mechanisms used by cells to respond to changes in their environment. Phosphorelays (of which two-component systems constitute a special case) are particularly abundant in prokaryotes and have been shown to be involved in many fundamental processes such as stress response, osmotic regulation, virulence, and chemotaxis. We develop a general model of phosphorelays extending existing models of phosphorelays and two-component systems. We analyze the model analytically under the assumption of mass-action kinetics and prove that a phosphorelay has a unique stable steady-state. Furthermore, we derive explicit functions relating stimulus to the response in any layer of a phosphorelay and show that a limited degree of ultrasensitivity in the bottom layer of a phosphorelay is an intrinsic feature which does not depend on any reaction rates or substrate amounts. On the other hand, we show how adjusting reaction rates and substrate amounts may lead to higher degrees of ultrasensitivity in intermediate layers. The explicit formulas also enable us to prove how the response changes with alterations in stimulus, kinetic parameters, and substrate amounts. Aside from providing biological insight, the formulas may also be used to replace the time-consuming simulations in numerical analyses.

© 2012 Elsevier Ltd. All rights reserved.

1. Introduction

Throughout the course of evolution, living organisms have developed a variety of different cellular mechanisms capable of responding to external stimulus, and post-translational modification of proteins is common to many of these mechanisms. In particular, modification by phosphorylation is widespread, and it is estimated that about 30% of all proteins undergo modification by phosphorylation (Cohen, 2000).

One particular type of phosphorylation mechanism is the so-called *phosphorelay* in which a phosphate group is transferred via a series of proteins through binding (Appleby and Parkinson, 1996; Perraud et al., 1999; Stock et al., 2000; West and Stock, 2001). Phosphorelays are particularly abundant in prokaryotes, although some of these systems have also been identified in eukaryotes. Common to all phosphorelays are two proteins, a histidine kinase (HK) and a response regulator (RR). Upon sensing external stimulus, a histidine residue on the HK autophosphorylates using ATP, and the phosphate group is transferred to an aspartate residue on the RR, either directly or through a series of intermediate steps. When phosphorylated, an output domain of the RR is capable of adjusting the cellular response.

Four examples of phosphorelays are shown in Fig. 1. The EnvZ/OmpR system in *Escherichia coli* is involved in osmoregulation of porin genes (Stock et al., 2000; Russo and Silhavy, 1991). Since it comprises only two components, the HK and the RR, it is also referred to as a *two-component system* (TCS). A slightly more complicated TCS example is the BvgS/BvgA system in *Bordetella pertussis*, used by the bacterium to activate virulence genes (Stock et al., 2000; Uhl and Miller, 1996; Cotter and Jones, 2003), where the HK contains three phosphorylation sites. Some systems have one or more intermediate phosphotransfer modules, as is e.g. the case for the osmoregulation pathway Sln1p/Ypd1p/Ssk1p in *Saccharomyces cerevisiae* (Stock et al., 2000; Maeda et al., 1994; Posas et al., 1996) and the sporulation initiating pathway Spo0A/Spo0F/Spo0B/Spo0A in *Bacillus subtilis* (Stock et al., 2000; Burbulys et al., 1991; Perego and Hoch, 1996; Hoch, 1993).

The phosphorelays mentioned above are among the most well-described examples in the literature, but they only constitute a small fraction of the several hundreds of phosphorelays known (Stock et al., 2000; Chang and Stewart, 1998), and studies of completed bacterial genomes have revealed the presence of many genes coding for HKs and RRs likely to be involved hitherto unknown phosphorelays (West and Stock, 2001; Zhang and Shi,
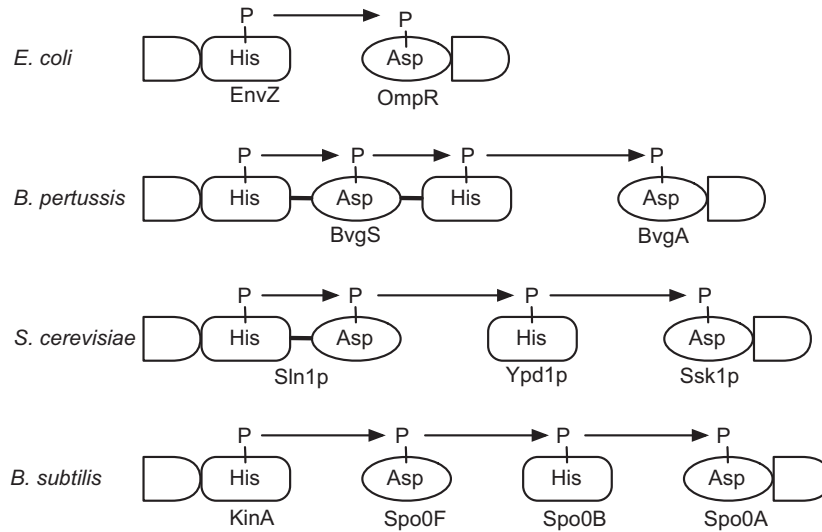

Fig. 1. Examples of phosphorelays with different architectures. The EnvZ/OmpR and BvgS/BvgA are both examples of TCSs, but they vary in the number of phosphorylation sites on the HK. The systems in *Saccharomyces cerevisiae* and *Bacillus subtilis* both have a total of four phosphorylation sites, but they are distributed on three and four proteins, respectively.

2005). For example, 62 such genes have been identified in *E. coli*, which amounts to more than 1% of the entire genome (West and Stock, 2001). Furthermore, the genes have been shown to be involved in a multitude of processes like stress response, osmotic regulation, virulence, and chemotaxis (Mizuno, 1997), which illustrates the importance and ubiquity of phosphorelays.

Given the widespread occurrence of phosphorelays, it is only natural to ask what the benefits of such an elaborate signaling mechanism are. Among the phosphorelays known today, none have more than four phosphorylation sites in total (Appleby and Parkinson, 1996; Stock et al., 2000). However, as illustrated in Fig. 1, the architectures may differ in the number of phosphorylation sites on each protein. One may thus speculate that whether the phosphorylation sites are located on one or more proteins influences the function of the phosphorelay, and that the benefits of a phosphorelay quickly saturate (or are balanced by drawbacks) with an increasing number of phosphorylation sites.

Mathematical modeling has been applied to study various types of biological networks e.g. enzymatic reaction networks (Gunawardena, 2007, 2005; Manrai and Gunawardena, 2008; Salazar and Höfer, 2007; Salazar, 2009; Thomson and Gunawardena, 2009a; Kapuy et al., 2009; Wang and Sontag, 2007) and signaling cascades (Goldbeter and Koshland, 1981, 1984; Huang and Ferrell, 1996; Feliu et al., 2012a; Blüthgen et al., 2006; Markevich et al., 2004; Ventura et al., 2008; Conradi et al., 2008), and has provided insight into steady-states, response to external stimulus, and robustness to changes in protein levels and kinetic parameters (Gunawardena, 2010; Shinar and Feinberg, 2010; Shinar et al., 2007; Li et al., 2004; Batchelor and Goulian, 2003; Barkai and Leibler, 1997). Precise measurements of concentrations and reaction rates are often difficult to obtain, and modeling can assist by determining whether e.g. the number of steady states and the qualitative stimulus–response behavior is intrinsic to the network architecture and not dependent on the actual concentrations and reaction rates.

Here we develop a general model of phosphorelays of any size and architecture based on mass-action kinetics. The model extends existing models of phosphorelays (Kim and Cho, 2006; Csikász-Nagy et al., 2011), and using an algebraic approach developed in Feliu et al. (2012a) we analytically analyze the model without resorting to numerical simulations. We prove the existe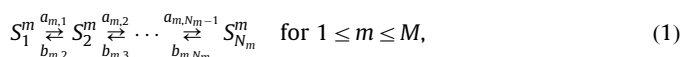nce of a unique stable steady-state and show how it varies with changing model parameters. Furthermore, we obtain explicit expressions for stimulus–response curves. This allows us to derive an upper bound on the response coefficient in the bottom layer of any phosphorelay irrespectively of size and architecture, which is in agreement with what has been observed in both experiments and numerical models (Csikász-Nagy et al., 2011; Fujita and Losick, 2005). Furthermore, we show that even for small phosphorelays (comprising only three phosphorylation sites), qualitatively very different response patterns are possible, and we derive explicit conditions on reaction rates and substrate concentrations describing each pattern. This contrasts what have previously been reported using simulation studies where saturation of phosphorylated sites at the bottom of the phosphorelay was suggested to cause a rise in response to sequentially propagate up through the phosphorelay (Csikász-Nagy et al., 2011).

Convergence and stability of the steady-state is proved using the theory of monotone dynamical systems (Angeli et al., 2010, 2007), which also provides the existence and uniqueness of the steady-state. However, our more direct algebraic approach to solving the steady-state equations is rewarded in that the calculations naturally extend to analytical results on the stimulus–response behavior. Combined with recent systematic approaches for reducing the complexity of the equations to be solved (Feliu and Wiuf, 2011; Thomson and Gunawardena, 2009b), we hope that similar direct, analytical calculations will become tractable for other chemical reaction networks too.

2. The model

We consider a general phosphorelay system consisting of $M \geq 2$ substrates $S^1, S^2, \ldots, S^M$, where the mth substrate S^m has $N_m \geq 1$ phosphorylation sites (see Fig. 2). We assume that substrates are never phosphorylated at more than one site at a time and denote by S_n^m the mth substrate phosphorylated at its nth site with $n=0$ corresponding to the unphosphorylated state. We refer to the set of all phosphoforms S_n^m with $0 \leq n \leq N_m$ as the mth *layer* of the phosphorelay and to N_m as the *length* of the mth layer.

We assume mass-action kinetics and that phosphate transfer within a substrate happens sequentially:

$$S_1^m \underset{b_{m,2}}{\overset{a_{m,1}}{\rightleftharpoons}} S_2^m \underset{b_{m,3}}{\overset{a_{m,2}}{\rightleftharpoons}} \cdots \underset{b_{m,N_m}}{\overset{a_{m,N_m-1}}{\rightleftharpoons}} S_{N_m}^m \quad \text{for } 1 \leq m \leq M, \qquad (1)$$
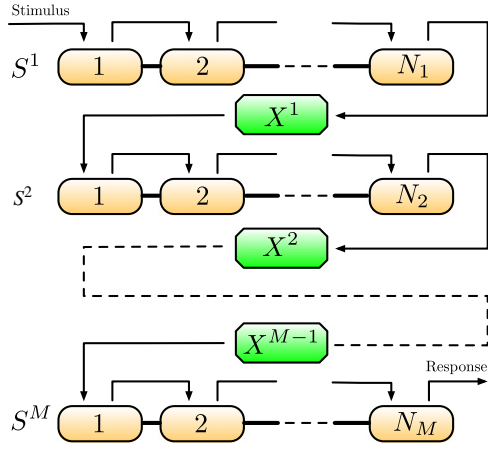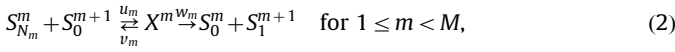
Fig. 2. Schematic illustration of a general phosphorelay comprising M layers. The number of phosphorylation sites in the mth layer is N_m, and the transfer of phosphate from one layer to the next is mediated via an intermediate complex.

with positive reaction constants $a_{m,n}$ and $b_{m,n}$, and we refer to these as *intralayer* reaction rates. The transfer of phosphate groups between substrates in two different layers is modeled via the formation of intermediate complexes:

$$S^m_{N_m} + S^{m+1}_0 \overset{u_m}{\underset{v_m}{\rightleftarrows}} X^m \overset{w_m}{\rightarrow} S^m_0 + S^{m+1}_1 \quad \text{for } 1 \le m < M, \tag{2}$$

with positive reaction constants u_m, v_m, and w_m. That is, only when S^m is phosphorylated at its last site can it transmit phosphate to the next layer.

Finally, we assume constant rates of phosphorylation (resp. dephosphorylation) of S^1_0 and $S^M_{N_M}$, respectively, represented by two reactions:

$$S^1_0 \overset{c}{\rightarrow} S^1_1 \quad \text{and} \quad S^M_{N_M} \overset{d}{\rightarrow} S^M_0. \tag{3}$$

The system is essentially linear with each new layer introducing a new substrate. However, the mechanism of phosphorylation in the top layer is different from the phosphotransfer mechanism between the subsequent layers. Similarly, dephosphorylation of the bottom layer is different from the dephosphorylation mechanism in the other layers, which is also phosphotransfer.

The *stimulus* activating the relay is implicitly captured in the reaction constant c. Increasing c corresponds to increasing the stimulus. When c is very low, most of the substrate S^1 will remain unphosphorylated, whereas higher values of c will push the substrate towards the phosphorylated phosphoforms. The *final response* $S^M_{N_M}$ transmits its phosphate group to a receptor molecule, and this is modeled as a loss of the phosphate group without details about other molecules potentially involved in the process.

To avoid cumbersome notation, we denote by S both the species S and its concentration. It should always be clear from the context what is meant. Under the assumption of mass-action kinetics, the reactions (1)–(3) give rise to a set of differential equations:

$$\dot{S}^1_0 = -cS^1_0 + w_1X^1,$$

$$\dot{S}^m_0 = -u_{m-1}S^{m-1}_{N_{m-1}}S^m_0 + v_{m-1}X^{m-1} + w_mX^m \quad 1 < m < M,$$

$$\dot{S}^M_0 = -u_{M-1}S^{M-1}_{N_{M-1}}S^M_0 + v_{M-1}X^{M-1} + dS^M_{N_M},$$

$$\dot{S}^1_1 = cS^1_0 - a_{1,1}S^1_1 + b_{1,2}S^1_2,$$

$$\dot{S}^m_1 = w_{m-1}X^{m-1} - a_{m,1}S^m_1 + b_{m,2}S^m_2 \quad 1 < m \le M,$$

$$\dot{S}^m_n = a_{m,n-1}S^m_{n-1} + b_{m,n+1}S^m_{n+1} - (b_{m,n} + a_{m,n})S^m_n,$$
$$\quad 1 \le m \le M, \quad 1 < n < N_m,$$

$$\dot{S}^m_{N_m} = -u_mS^m_{N_m}S^{m+1}_0 + v_mX^m + a_{m,N_m-1}S^m_{N_m-1} - b_{m,N_m}S^m_{N_m} \quad 1 \le m < M,$$

$$\dot{S}^M_{N_M} = a_{M,N_M-1}S^M_{N_M-1} - (b_{M,N_M} + d)S^M_{N_M},$$

$$\dot{X}^m = u_mS^m_{N_m}S^{m+1}_0 - (v_m + w_m)X^m \quad 1 \le m < M,$$

By direct inspection it follows that

$$\dot{S}^m_0 + \dot{S}^m_1 + \cdots + \dot{S}^m_{N_m} + \dot{X}^{m-1} + \dot{X}^m = 0, \tag{4}$$

for all $1 \le m \le M$, where we have defined $X^0 = X^M = 0$ in order to simplify notation, and hence the sum:

$$S^m_{tot} = S^m_0 + S^m_1 + \cdots + S^m_{N_m} + X^{m-1} + X^m, \tag{5}$$

is conserved for all $1 \le m \le M$. This reflects the fact that S^m either exists in one of its $N_m + 1$ phosphoforms or is bound in one of the intermediate complexes X^{m-1} or X^m. We will refer to S^m_{tot} as the *total amount* of the substrate S^m and to (5) as the *conservation law* for S^m.

In the following section we prove that for fixed reaction constants and total amounts of substrate, the phosphorelay has a unique steady-state, and we use the insight obtained in the proof to investigate the stimulus–response behavior of the system.

3. Results

3.1. Steady-state equations

The steady-state equations are the differential equations equated to zero along with the conservation laws for positive total amounts S^m_{tot}, and the steady-states are found by solving these for the variables (substrate phosphoforms and intermediate complexes). Hence there is a steady-state equation corresponding to each species as well as M additional conservation laws. Since there are $M-1$ intermediate complexes, and each substrate S^m exists in $N_m + 1$ different phosphoforms, it follows that the system consists of $3M-1 + \sum_{m=1}^M N_m$ equations in $2M-1 + \sum_{m=1}^M N_m$ variables.

To obtain a simpler system of equations that more clearly elucidates the constraints imposed by the phosphorelay structure, we manipulate the steady-state equations to obtain a simpler, but equivalent, set of equations.

First note that according to (4), the equations $\dot{S}^m_1 = 0$ for $1 \le m \le M$ hold if $\dot{S}^m_n = 0$ and $\dot{X}^m = 0$ hold for all m and $n \ne 1$, and we may therefore leave them out. For all $1 \le m < M$, the steady-state equation $\dot{X}^m = 0$ is equivalent to the equation $\dot{X}^m + \dot{S}^{m+1}_0 = 0$, which in turn is equivalent to

$$X^m = \frac{d}{w_m}S^M_{N_M} \quad \text{for } 1 \le m < M. \tag{6}$$

Furthermore, by replacing all $\dot{S}^m_{N_m} = 0$ by the equivalent $\dot{S}^m_{N_m} - \dot{S}^{m+1}_0 = 0$, it follows after inserting (6) that this is equivalent to

$$S^m_{N_m-1} = \frac{b_{m,N_m}S^M_{N_M} + dS^M_{N_M}}{a_{m,N_m-1}} \quad \text{for } 1 \le m \le M. \tag{7}$$

For $1 \leq n < N_m - 1$, the steady-state equation $\dot{S}_{n+1}^m = 0$ is equivalent to

$$S_n^m = \frac{(a_{m,n+1} + b_{m,n+1})S_{n+1}^m - b_{m,n+2}S_{n+2}^m}{a_{m,n}} \quad \text{for } 1 \leq m \leq M, \qquad (8)$$

and using induction, we may combine (7) and (8) in one equivalent statement,

$$S_n^m = \frac{B_{m,n}S_{N_m}^m + dC_{m,n}S_{N_M}^M}{A_{m,n}} \quad \text{for } \begin{array}{l} 1 \leq m \leq M \\ 1 \leq n \leq N_m, \end{array} \qquad (9)$$

where the constants are defined by

$$A_{m,n} = \prod_{i=n}^{N_m-1} a_{m,i}, \quad B_{m,n} = \prod_{i=n+1}^{N_m} b_{m,i},$$

$$C_{m,n} = \sum_{i=n+1}^{N_m} \left(A_{m,i} \prod_{j=n+1}^{i-1} b_{m,j} \right) \qquad (10)$$

for $1 \leq m \leq M$ and $0 \leq n \leq N_m$. In particular, these definitions imply that $A_{m,N_m} = B_{m,N_m} = 1$, $C_{m,N_m} = 0$, and $C_{m,N_m-1} = 1$. Apart from C_{m,N_m}, the constants are all positive and depend only on the intralayer reaction constants $a_{m,n}$ and $b_{m,n}$ in the mth layer.

Using (6) and (9), we see that the conservation law (5) is fulfilled if and only if

$$S_0^m = S_{tot}^m - \lambda_m S_{N_M}^M - \mu_m S_{N_m}^m \quad \text{for } 1 \leq m \leq M, \qquad (11)$$

with constants given by

$$\lambda_m = d\left(\frac{1}{w_{m-1}} + \frac{1}{w_m} + \sum_{n=1}^{N_m} \frac{C_{m,n}}{A_{m,n}} \right) \quad \text{and} \quad \mu_m = \sum_{n=1}^{N_m} \frac{B_{m,n}}{A_{m,n}} \qquad (12)$$

(terms involving the undefined rates w_0 and w_M are removed). The constants are all positive and depend only on reaction rates in the mth and $(m-1)$th layer. Finally, using (6) it follows that $\dot{S}_0^m = 0$ is equivalent to

$$cS_0^1 = dS_{N_M}^M \quad \text{and} \quad d\left(\frac{v_{m-1}}{w_{m-1}} + 1 \right)S_{N_M}^M = u_{m-1}S_{N_{m-1}}^{m-1}S_0^m \quad \text{for } 1 < m \leq M.$$

Summing up, the set of steady-state equations are replaced by an equivalent set of equations:

(**SS1**) $cS_0^1 = dS_{N_M}^M$,

(**SS2**) $X^m = \dfrac{d}{w_m}S_{N_M}^M \quad 1 \leq m < M$,

(**SS3**) $S_n^m = \dfrac{B_{m,n}S_{N_m}^m + dC_{m,n}S_{N_M}^M}{A_{m,n}} \quad 1 \leq m \leq M, \ 1 \leq n \leq N_m$,

(**SS4**) $S_0^m = S_{tot}^m - \lambda_m S_{N_M}^M - \mu_m S_{N_m}^m \quad 1 \leq m \leq M$,

(**SS5**) $d\left(\dfrac{v_{m-1}}{w_{m-1}} + 1 \right)S_{N_M}^M = u_{m-1}S_{N_{m-1}}^{m-1}S_0^m \quad 1 < m \leq M$,

with constants defined in (10) and (12). Note that the reaction rate c only appears in (**SS1**).

Throughout this paper we assume that all reaction constants and total amounts are fixed and positive unless otherwise clearly stated. Any solution to the steady-state equations is a steady-state, and the system could therefore possess multiple steady-states, some of which with negative concentrations. These are not biologically obtainable, so the focus is on steady-states in which all concentrations are non-negative (zero or positive). We call these *biologically meaningful steady-states* (BMSSs).

3.2. Existence of a unique stable BMSS

In this section we prove the existence of a unique stable BMSS for a general phosphorelay. We do so by writing all steady-state concentrations as rational functions of the final response $S_{N_M}^M$ (recall that a *rational function* in x is a quotient $f(x)/g(x)$ of two polynomial functions in x) and then show that precisely one value of $S_{N_M}^M$ gives rise to a BMSS.

Starting with the Mth layer, we work our way to the top layer by layer. The link between layers is obtained by relating the steady-state value of $S_{N_m}^m$ with that of $S_{N_M}^M$ through a rational function $S_{N_m}^m = \psi_m(S_{N_M}^M)$. The singularities of ψ_m for $1 \leq m \leq M$ provide a necessary condition $S_{N_M}^M < \xi_m$ for non-negative concentrations in the layers $m, m+1, \ldots, M$, and we prove that $\xi_1 < \xi_2 < \cdots < \xi_{M-1}$, from which it follows that $S_{N_M}^M < \xi_1$ is necessary for all concentrations to be positive. We then write $c = \psi_0(S_{N_M}^M)$ as an increasing rational function of $S_{N_M}^M$ and demonstrate how this leads to a stronger necessary condition $S_{N_M}^M < \xi_0$. Finally, we show that for any given value of c, the equation $c = \psi_0(S_{N_M}^M)$ has a unique solution $S_{N_M}^M$ in $[0, \xi_0)$, which establishes the existence and uniqueness of a BMSS. In fact, it turns out that all steady-state concentrations are strictly positive.

Note that (**SS2**)–(**SS4**) express X^m and S_n^m for $0 \leq n \leq N_m$ as rational functions of $S_{N_M}^M$ and $S_{N_m}^m$ with coefficients depending on the intralayer reaction constants in the mth layer and the reaction constants d, w_m, and w_{m-1} only. We now show how (**SS5**) yields the link to express all $S_{N_m}^m$ as rational functions of $S_{N_M}^M$.

We first show that at steady-state $S_0^m \neq 0$ for all $1 \leq m \leq M$. If this is not the case, there is a largest m for which $S_0^m = 0$, and (**SS5**) then implies that $S_{N_M}^M = 0$. For $m = M$, (**SS4**) implies that $S_{tot}^M = 0$, which contradicts the assumption of positive total amounts. For $m < M$ we argue as follows: Since m is the largest with the property $S_0^m = 0$, we have $S_0^{m+1} \neq 0$, and combined with $S_{N_M}^M = 0$, it follows from (**SS5**) that $S_{N_m}^m = 0$. Now using (**SS4**) yields $S_{tot}^m = 0$, which again contradicts the assumption of positive total amounts.

Since S_0^m is non-zero at steady-state, we may isolate $S_{N_{m-1}}^{m-1}$ in (**SS5**) and use (**SS4**) to get

$$S_{N_{m-1}}^{m-1} = \frac{d\left(\dfrac{v_{m-1}}{w_{m-1}} + 1 \right)S_{N_M}^M}{u_{m-1}(S_{tot}^m - \lambda_m S_{N_M}^M - \mu_m S_{N_m}^m)} \quad \text{for } 1 < m \leq M, \qquad (13)$$

which shows that if we define ψ_m recursively by $\psi_M = \mathrm{id}$, and

$$\psi_{m-1}(y) = \frac{d\left(\dfrac{v_{m-1}}{w_{m-1}} + 1 \right)y}{u_{m-1}(S_{tot}^m - \lambda_m y - \mu_m \psi_m(y))} \quad \text{for } 1 < m \leq M, \qquad (14)$$

then $\psi_m(S_{N_M}^M) = S_{N_m}^m$ at steady-state. The recursive definition implies that ψ_m is a rational function. Furthermore, by isolating c in (**SS1**) and inserting S_0^1 from (**SS4**), it follows using $S_{N_1}^1 = \psi_1(S_{N_M}^M)$ that $c = \psi_0(S_{N_M}^M)$, where

$$\psi_0(y) = \frac{dy}{S_{tot}^1 - \lambda_1 y - \mu_1 \psi_1(y)} \qquad (15)$$

is also a rational function.

Writing $\psi_M(y) = p_M(y)/q_M(y)$ with $p_M(y) = y$ and $q_M(y) = 1$, we may use (14) and (15) to recursively write all $\psi_m(y)$ as quotients $p_m(y)/q_m(y)$ with $p_m(0) = 0$, where both p_m and q_m are polynomials of degree $M - m$ for all $0 \leq m < M$.

Proposition 3.1. *The steady-state equations (**SS1**)–(**SS5**) are satisfied, if and only if (**SS2**)–(**SS4**) are satisfied along with $\psi_0(S_{N_M}^M) = c$, and $\psi_m(S_{N_M}^M) = S_{N_m}^m$ for all $1 \leq m \leq M$.*

Furthermore, for all $m < M$ the function ψ_m has a minimal positive singularity ξ_m satisfying

$$\xi_{M-1} > \xi_{M-2} > \cdots > \xi_1 > \xi_0 > 0.$$

Let $\xi_M = \xi_{M+1} = \infty$. Then ψ_m is continuous, non-negative and strictly increasing on $[0, \xi_m)$, negative on (ξ_m, ξ_{m+1}), and it satisfies $\psi_m(0) = 0$ and $\psi_m(y) \to \infty$ for $y \to \xi_m^-$ for all $0 \le m \le M$.

Proof. The first part of the proposition follows immediately since the equations $\psi_0(S_{N_M}^M) = c$ and $\psi_m(S_{N_M}^m) = S_{N_m}^m$ are just rearrangements of (**SS1**) and (**SS5**), respectively.

For the second part, the case $m = M$ is trivial since $\psi_M = \text{id}$, and (ξ_M, ξ_{M+1}) is the empty set. Assume now that the claim is true for $m + 1$ and consider the case m. By induction, ψ_{m+1} is increasing on $[0, \xi_{m+1})$, so the denominator of ψ_m is continuous and decreasing on $[0, \xi_{m+1})$, and it diverges towards $-\infty$ for $y \to \xi_{m+1}^-$. Therefore it has a unique zero $\xi_m < \xi_{m+1}$. Furthermore, the numerator of ψ_m is continuous and increasing and equals 0 for $y = 0$, and therefore the entire fraction $\psi_m(y)$ is continuous, positive, and increasing on $[0, \xi_m)$, negative on (ξ_m, ξ_{m+1}), $\psi_m(0) = 0$, and $\psi_m(y) \to \infty$ for $y \to \xi_m^-$. $\square$

Theorem 3.2. *For any set of fixed positive reaction constants and total amounts, the phosphorelay converges to a unique stable BMSS. In fact, the steady-state concentrations of all substrates and intermediate complexes are positive.*

Proof. It follows from Proposition 3.1 that $S_{N_m}^m \ge 0$ at steady-state, if and only if $S_{N_M}^M$ is in $[0, \xi_m)$, and since $\xi_1 < \xi_2 < \cdots < \xi_{M-1}$, it follows that $S_{N_M}^M < \xi_1$ is a necessary condition for a BMSS. According to (**SS2**), we have $X^m \ge 0$ for $1 \le m \le M$ for any $S_{N_M}^M \ge 0$, and by inserting $S_{N_m}^m \ge 0$ into (**SS3**), it shows that also $S_n^m \ge 0$ for all $1 \le m \le M$ and $1 \le n < N_m$. Finally, because ξ_m by definition is the smallest positive root of the right-hand side of (**SS4**) after substituting $S_{N_m}^m = \psi_m(S_{N_M}^M)$, it follows that $S_0^m > 0$ for all $1 \le m \le M$. The argument also implies that all steady-state concentrations are positive if and only if $S_{N_M}^M > 0$, and since $\psi_0(S_{N_M}^M) = c > 0$, this is always the case.

According to Proposition 3.1, the function ψ_0 is continuous and increases from 0 to ∞ on $[0, \xi_0)$ and is negative on (ξ_0, ξ_1). It follows (see also Fig. 3) that precisely one value of $S_{N_M}^M$ in $[0, \xi_0)$ satisfies the condition $c = \psi_0(S_{N_M}^M)$. This establishes the existence and uniqueness of a BMSS.

The convergence and stability part can be proved using methods from the theory of monotone dynamical systems (see

Fig. 3. The graph of ψ_0 for a three-layer phosphorelay with all reaction constants equal to one and all total amounts equal to ten.

Theorem 2 in Angeli et al., 2010), and a proof is included in Appendix C. $\square$

The proof of convergence and stability in Appendix C also implies existence and uniqueness of a BMSS, but the proof is not constructive and does not yield the additional insight provided by the functions ψ_m. On the other hand, our approach does not address the convergence to and the stability of the steady-state, and the two methods thus complement each other.

Additionally, this system fulfills the graphical conditions for injectivity of systems with outflow or degrading reactions stated in Banaji and Craciun (2010). This implies that the system admits at most one *non-degenerate* equilibrium for any kinetics belonging to the broad class of kinetics defined in Banaji and Craciun (2010), which includes for instance Hill-type kinetics.

4. Stimulus–response

In this section we demonstrate how the functions ψ_m may be used to explicitly describe stimulus–response behavior.

4.1. Maximal response

Let all total amounts and all reaction constants but the stimulus c be fixed. According to (15), the stimulus is an increasing continuous function of the response in $[0, \xi_0)$ and hence, *vice versa*, the response is an increasing continuous function of the stimulus. Furthermore, $S_{N_M}^M \to \xi_0$ for $c \to \infty$, and therefore ξ_0 is the smallest upper limit on all possible responses. The limit is not attainable but can be thought of as the response in a fictitious system with infinite stimulus, and we will refer to it as the *maximal response* of the phosphorelay.

As argued in Section 3.2, the rational function ψ_0 is the ratio of two polynomials of degree M, and calculating the maximal response is thus equivalent to finding the smallest positive root in a polynomial of degree M.

More generally, in a phosphorelay with all total amounts and all reaction rates but c fixed, we denote by ρ_m the smallest upper limit of all possible steady-state values of $S_{N_m}^m$ and call it the *maximal response* in the mth layer. We have just argued that $\rho_M = \xi_0$, and since according to Proposition 3.1 all ψ_m are increasing functions on intervals containing $[0, \xi_0)$, we have

$$\rho_m = \psi_m(\rho_M) \quad \text{for all } 1 \le m < M. \tag{16}$$

Since ψ_m is invertible (it is increasing and continuous), we have that $S_{N_M}^M = \psi_m^{-1}(S_{N_m}^m)$, and by substituting this into (14) we obtain

$$c = (\psi_0 \circ \psi_m^{-1})(S_{N_m}^m) \quad \text{for all } 1 \le m \le M, \tag{17}$$

which is the stimulus expressed as a function of the response in the mth layer. Note that since (17) involves the inverse of a rational function, it is, in general, not itself a rational function.

The explicit stimulus–response relationship may be used to investigate how changes in one layer m_0 are reflected in the maximal responses in all layers of a phosphorelay. Suppose that λ_{m_0} or μ_{m_0} is increased by changing reaction rates or by adding more phosphorylation sites to the substrate S^{m_0} in an existing layer (see (12)). Then the maximal response decreases (resp. increases) in layers below (resp. above) m_0. Increasing the total amount $S_{tot}^{m_0}$ has the opposite effect. Then the maximal response increases (resp. decreases) in layers downstream (resp. upstream) from layer m_0. This is illustrated for $M = 5$ in Fig. 4A, and proofs of both claims are given in Proposition A.1. The responses $S_{N_m}^m$ themselves exhibit the same behavior, and a proof of this is included in Proposition A.2. Summing up, these results enable us
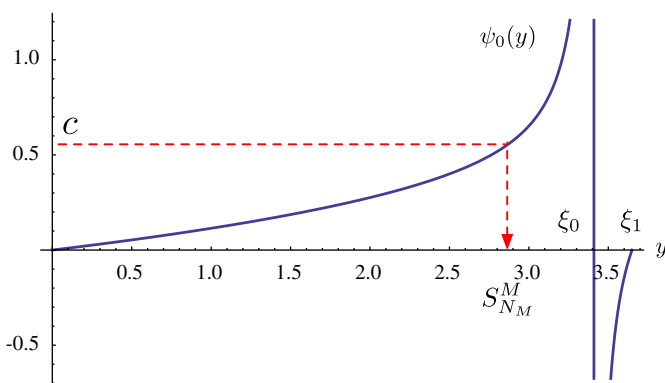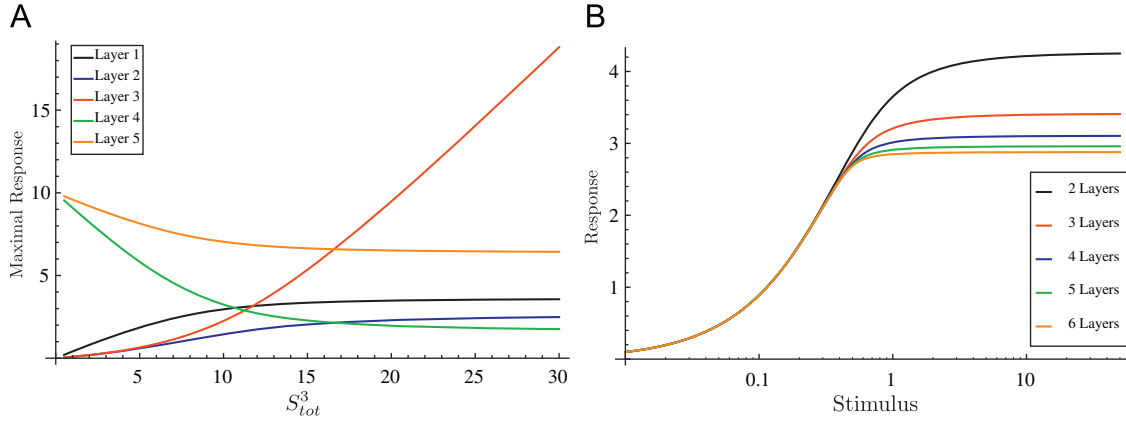
Fig. 4. (A) Maximal responses in all layers of a five-layer phosphorelay as functions of S_{tot}^3. When S_{tot}^3 increases, the maximal response increases in layers 1, 2, and 3, but decreases in layers 4 and 5. (B) Stimulus–response curves for the bottom layer in phosphorelays with 6, 5, 4, 3, and 2 layers, where smaller systems are obtained from larger by removal of upper layers. All reaction rates are set to one, and all total amounts are set to 10.
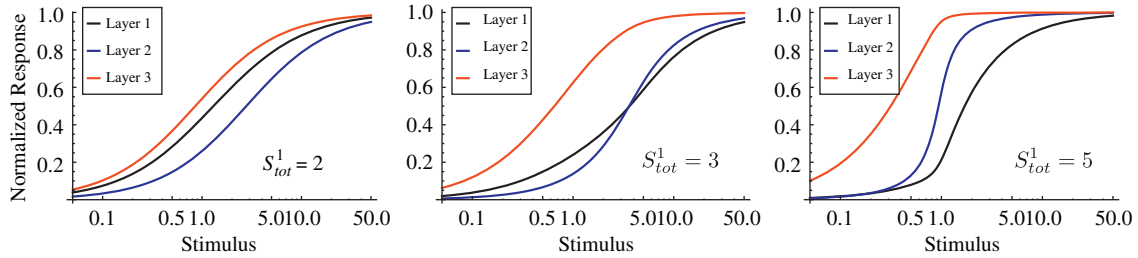

Fig. 5. Normalized stimulus–response curves for a three-layer phosphorelay with one phosphorylation site at each layer. Here $S_{tot}^2 = 20$, $S_{tot}^3 = 5$, and all reaction rates are set to one. Then $\varepsilon^* = 35/\rho_3 - 15$, where ρ_3 depends on S_{tot}^1, and by varying S_{tot}^1 we obtain three qualitatively different behaviors of the normalized response curves. The stimulus is on logarithmic scale.

to predict how all layers in the phosphorelay respond to changes in kinetic parameters and total amounts.

By removing the top layer from the system and adding a new stimulus reaction $S_0^2 \xrightarrow{c} S_1^2$, we obtain a smaller phosphorelay with $M-1$ layers, and its maximal final response is the minimal, positive zero of $S_{tot}^2 - \lambda_2 y - \mu_2 \psi_2(y)$, which is exactly ξ_1 from Proposition 3.1. In general, removing m layers from the original system results in a smaller system with a larger maximal final response equal to ξ_m, and this is illustrated for $M=6$ in Fig. 4B. With m layers removed, the phosphorylation $S_0^{m+1} \xrightarrow{c} S_1^{m+1}$ is direct, whereas in the larger system, some of the $S_{N_M}^m$ taking part in the phosphorylation (phosphotransfer) is sequestered in the intermediate complex X^m.

4.2. Ultrasensitive response

In this section we use the functions ψ_m to describe how steady-state concentrations respond to changes in stimulus. For any $0 < \varepsilon < 1$, we denote by $c_{m,\varepsilon}$ the amount of stimulus needed in order to obtain ε times the maximal response in the mth layer. That is, using the notation introduced in (16), we have

$$c_{m,\varepsilon} = (\psi_0 \circ \psi_m^{-1})(\varepsilon\rho_m) = \psi_0(\psi_m^{-1}(\varepsilon\psi_m(\rho_M))).$$

The *normalized response* in the mth layer is the response $S_{N_m}^m$ divided by its maximal value ρ_m, and plotted as a function of c we refer to it as the *normalized stimulus–response curve* for the mth layer. The curve consists of the points $(c_{m,\varepsilon}, \varepsilon)$ for $0 \le \varepsilon \le 1$, that is ε is the normalized response.

Proposition 4.1. *For all $m < M$ and $0 < \varepsilon < 1$ we have $c_{M,\varepsilon} < c_{m,\varepsilon}$. That is, the normalized stimulus–response curve for the bottom layer*

is shifted to the left of the normalized stimulus–response curves for all other layers.

The proof uses induction on m and it is given in Proposition A.3. The result in Proposition 4.1 cannot be extended to compare arbitrary layers, and we now demonstrate how it already fails for $M=3$. In fact, it turns out that, depending on the reaction rates and total amounts, we can have $c_{1,\varepsilon} > c_{2,\varepsilon}$ or $c_{1,\varepsilon} < c_{2,\varepsilon}$ for all $0 < \varepsilon < 1$, and in some cases the normalized stimulus–response curves for layers one and two intersect as illustrated in Fig. 5. Since ψ_1 and ψ_0^{-1} are increasing functions, comparing $c_{1,\varepsilon}$ and $c_{2,\varepsilon}$ is equivalent to comparing:

$$(\psi_1 \circ \psi_0^{-1})(c_{1,\varepsilon}) = \varepsilon\psi_1(\rho_3) \quad \text{and} \quad (\psi_1 \circ \psi_0^{-1})(c_{2,\varepsilon}) = \psi_1(\psi_2^{-1}(\varepsilon\psi_2(\rho_3))), \tag{18}$$

so it follows that comparing $c_{1,\varepsilon}$ and $c_{2,\varepsilon}$ is equivalent to determining the sign of $\Delta(\varepsilon) = \varepsilon\psi_1(\rho_3) - \psi_1(\psi_2^{-1}(\varepsilon\psi_2(\rho_3)))$. The expressions in (18) are easier to work with than the original ones, since we may calculate them explicitly. The maximal response ρ_3 is a root of a quadratic polynomial, and ψ_2^{-1} may be obtained directly, since ψ_2 is the ratio of two first degree polynomials.

By manipulating $\Delta(\varepsilon)$ (see Appendix B for details), we see that its sign is determined by the roots of a polynomial of degree three in ε. We find that both 0 and 1 are roots, and the third root is

$$\varepsilon^* = \frac{w_2 u_2(S_{tot}^2(\lambda_3 + \mu_3) - \lambda_2 S_{tot}^3)(S_{tot}^3 - (\lambda_3 + \mu_3)\rho_3) - d(v_2 + w_2)\mu_2 S_{tot}^3}{du_1(v_2 + w_2)\mu_2(\lambda_3 + \mu_3)\rho_3}.$$

It depends both on the reaction rates and the total amounts and may be calculated explicitly. We find that if $\varepsilon^* < 0$ (resp. $\varepsilon^* > 1$), then $c_{1,\varepsilon} > c_{2,\varepsilon}$ (resp. $c_{1,\varepsilon} < c_{2,\varepsilon}$) for all $0 < \varepsilon < 1$, whereas if

$0 < \varepsilon^* < 1$, the normalized stimulus–response curves intersect for $\varepsilon = \varepsilon^*$, and $c_{1,\varepsilon} > c_{2,\varepsilon}$ (resp. $c_{1,\varepsilon} < c_{2,\varepsilon}$) for $\varepsilon < \varepsilon^*$ (resp. $\varepsilon > \varepsilon^*$).

We now continue our general investigation of how steady-state concentrations respond to changes in stimulus. For $0 < \varepsilon < \delta < 1$, we consider the *response coefficient*:

$$\chi_{m,\varepsilon,\delta} = \frac{c_{m,\varepsilon}}{c_{m,\delta}} \quad \text{for } 1 \le m \le M, \tag{19}$$

which relates the amount of stimulus required to obtain ε (resp. δ) times the maximal possible response in the mth layer. Since the response in any layer is an increasing function of the stimulus, it follows that

$$0 < \chi_m < 1 \quad \text{for } 1 \le m \le M.$$

Often one puts $\varepsilon = 0.1$ and $\delta = 0.9$, and in the literature, systems with $\chi_{m,0.1,0.9} > 1/81$ are commonly referred to as *ultrasensitive* (Goldbeter and Koshland, 1981). This is illustrated in a five-layer example in Fig. 6, where the intermediate layers (in particular the third) exhibit ultrasensitive behaviors. On the other hand, the top layer shows an almost linear increase in response before reaching a plateau.

Proposition 4.2. *For a general M-layer phosphorelay we have* $\chi_{M,\varepsilon,\delta} < \varepsilon/\delta$.
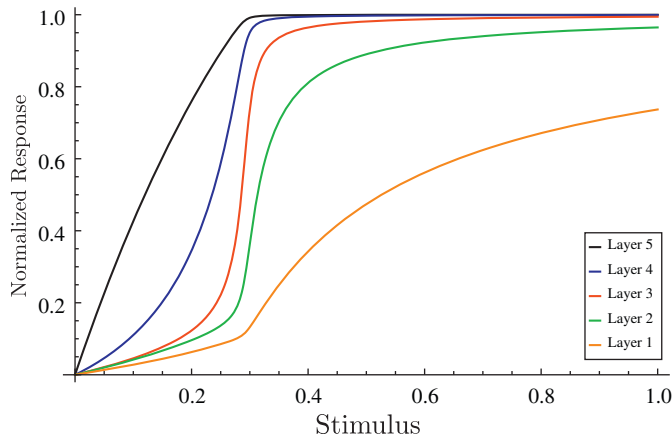

Fig. 6. Normalized stimulus–response curves for a five-layer phosphorelay with one phosphorylation site at each layer. Here $S_{tot}^1 = S_{tot}^2 = S_{tot}^3 = S_{tot}^4 = 10$, $S_{tot}^5 = 5$, and all reaction rates are set to one. The response in the top layer increases almost linearly before it reaches a plateau. The third layer shows an ultrasensitive behavior.
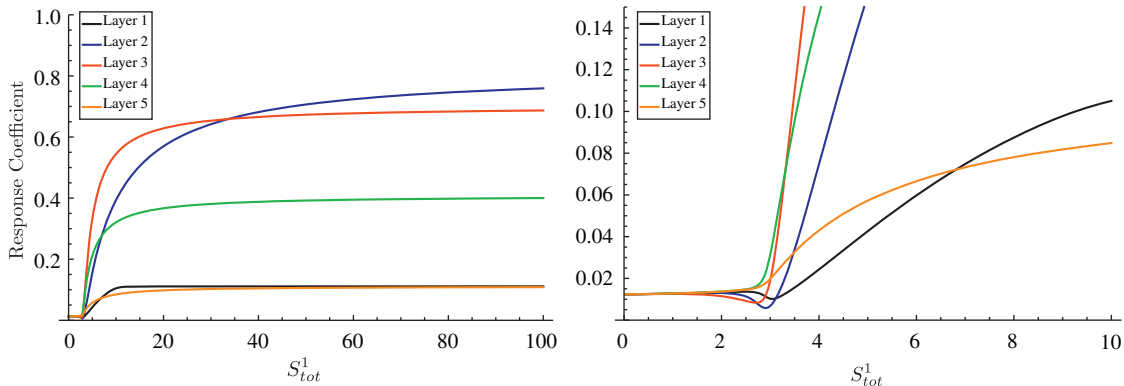
Proof. It follows immediately by using (15) that

$$\chi_{M,\varepsilon,\delta} = \frac{c_{M,\varepsilon}}{c_{M,\delta}} = \frac{\varepsilon}{\delta} \cdot \frac{S_{tot}^1 - \lambda_1 \delta \rho_M - \mu_1 \psi_1(\delta \rho_M)}{S_{tot}^1 - \lambda_1 \varepsilon \rho_M - \mu_1 \psi_1(\varepsilon \rho_M)},$$

and since $\psi_1(y)$ according to Proposition 3.1 is an increasing function, it follows that in the second fraction, the numerator is smaller than the denominator, and this proves the claim. □

The result in Proposition 4.2 shows that for any set of reaction rates and total amounts, the degree of ultrasensitivity in the bottom layer is bounded by the same constant ($\chi_{M,0.1,0.9} < 1/9$), and this is thus an intrinsic feature of the phosphorelay.

We are unaware whether the response coefficients $\chi_{m,\varepsilon,\delta}$ are bounded for general m. Numerical experiments indicate that also $\chi_{1,\varepsilon,\delta} < \varepsilon/\delta$, but we have not been able to determine this analytically. However, it is possible to calculate the response coefficients in some limit cases, for example when the total amount S_{tot}^1 in the top layer is increased or decreased, which could e.g. be used in an experimental setup where S_{tot}^1 can be controlled. The proof of Proposition 4.3 below is given in Appendix A.

Proposition 4.3. *Let $1 \le m \le M$ and $1 < \varepsilon < \delta < 1$, and let all reaction constants and all total amounts except S_{tot}^1 be fixed. Then*

$$\chi_{m,\varepsilon,\delta} \to \frac{\varepsilon(1-\delta)}{\delta(1-\varepsilon)} \quad \text{for } S_{tot}^1 \to 0$$

$$\chi_{m,\varepsilon,\delta} \to \begin{cases} \dfrac{1-\delta}{1-\varepsilon} & \text{if } m = 1 \\[2ex] \dfrac{\psi_m^{-1}(\varepsilon \psi_m(\xi_1))}{\psi_m^{-1}(\delta \psi_m(\xi_1))} & \text{if } 1 < m < M \quad \text{for } S_{tot}^1 \to \infty, \\[2ex] \dfrac{\varepsilon}{\delta} & \text{if } m = M \end{cases}$$

and $\psi_m^{-1}(\varepsilon \psi_m(\xi_1))/\psi_m^{-1}(\delta \psi_m(\xi_1)) > \varepsilon/\delta$.

For $\varepsilon = 0.1$ and $\delta = 0.9$, the limit $[\varepsilon(1-\delta)]/[\delta(1-\varepsilon)]$ is $1/81$, the common threshold for ultrasensitivity, and for sufficiently high S_{tot}^1, the intermediate layers will exhibit higher degrees of ultrasensitivity than the bottom layer. Note that the limits are not necessarily global bounds on the response coefficients as illustrated in Fig. 7.

5. Discussion

In this paper we have introduced and analytically analyzed a general model of phosphorelays, which extends existing models of phosphorelays (Kim and Cho, 2006; Csikász-Nagy et al., 2011), and we have proved the existence and uniqueness of a steady-state. Furthermore, we have derived explicit formulas for the

Fig. 7. Response coefficients for a five-layer phosphorelay with one phosphorylation site at each layer. Here $S_{tot}^2 = S_{tot}^3 = S_{tot}^4 = 10$, $S_{tot}^5 = 5$, and all reaction rates are set to one. The second plot emphasizes the behavior for small values of S_{tot}^1 and reveals that response coefficients are not necessarily increasing functions of S_{tot}^1.

responses in all layers as functions of the stimulus and used these to investigate various aspects of the stimulus–response behavior.

We have showed that the response coefficient in the bottom layer of any phosphorelay is bounded by constants independent of size and architecture of the phosphorelay. Furthermore, we have also demonstrated how qualitatively very different stimulus–response behaviors are possible in layers above the last, and in the three-layer case we have derived an exact condition which distinguishes the three possible scenarios in that case. The variety of behaviors contrasts what has been reported in previous studies using numerical simulations (Csikász-Nagy et al., 2011).

The finding that the response coefficient in the bottom layer is bounded is consistent with experimental findings. For example, in the four-layer phosphorelay involved in sporulation initiation of *B. subtilis* (see Fig. 1), it has been observed that the response (the concentration of Spo0A $\sim$ P) is only gradually increasing with the stimulus (Fujita and Losick, 2005). It has been shown that Spo0A $\sim$ P directly regulates over 100 genes, and that these are activated and repressed at very different concentrations of Spo0A $\sim$ P (Molle et al., 2003). A possible explanation of the gradual response observed in Fig. 6 could therefore be that important gene products, transcribed only at intermediate concentrations of Spo0A $\sim$ P, would otherwise be produced in too low concentrations to trigger sporulation. This would be the case if phosphorylation of Spo0A happens too fast and the system therefore fails to spend the required time in the intermediate states. However, other factors might contribute, for example cross-talk between pathways and interplay between competing kinases. The Spo0A pathway is known to involve at least three different HKs (KinA, KinB, and KinC) and we do not model either of these effects.

Ultrasensitivity in intermediate layers has previously been suggested using a simpler model (Csikász-Nagy et al., 2011), but to our knowledge no experimental studies have determined whether or not this happens *in vitro*. The presence of intermediate layers allows for additional control of the response, where e.g. an increase in stimulus my be counteracted upon by removal of phosphate in an intermediate layer. For example, there are phosphatases RapA, RapB, and RapE, which are known to dephosphorylate Spo0F $\sim$ P, and Spo0E which is known to dephosphorylate Spo0A $\sim$ P (Perego and Hoch, 1996; Saito, 2001; Ohlsen et al., 1994). We speculate that the ultrasensitivity in intermediate layers is essential for precise control of cross-talk with external pathways.

We have argued that as the number of layers is increased, the maximal final response decreases. In the example in Fig. 4, the effect appears to saturate already for five layers, a feature not specific to the selected values of reaction constants and total amounts. In fact, the saturation is often observed even earlier. This suggest that the saturation is an intrinsic feature of the phosphorelay structure itself and not the specific reaction rates and total amounts. This fits with the fact that all known phosphorelays to this day contain at most four sites (Appleby and Parkinson, 1996).

Our model is a simplified model that does not take case-specific features of phosphorelays and TCSs into account. For example, there are HKs which act as phosphatases on their cognate RRs. Such bifunctional HKs have almost exclusively been observed in TCSs, and we do not model them in our general phosphorelay model. The consequences of having bifunctional HKs in general phosphorelays has been shown to result in a flattening of the stimulus–response curves (Csikász-Nagy et al., 2011).

This paper demonstrates that even relatively complicated systems such as phosphorelays may be treated analytically. Important features of chemical reaction networks may be overlooked if one resorts to numerical simulations alone. Using our approach, previously developed and applied to signaling cascades and enzymatic reactions (Feliu et al., 2012a, 2012b; Feliu and Wiuf, in press), we are able to derive exact and qualitative results about steady-states and stimulus–response behavior for any phosphorelay independent of the number and length of layers, reaction constants, and total amounts of substrate. Also this approach, by providing simple (recursive) expressions relating species concentrations at steady-state, allows for fast and efficient numerical analysis thereby avoiding computationally demanding and error-prone calculations of e.g. steady-state values.

Acknowledgments

Appendix A. Proofs

Proposition A.1. *If λ_{m_0} or μ_{m_0} is increased, or if the total amount of substrate $S_{tot}^{m_0}$ is decreased, then the maximal response decreases in layers $m \geq m_0$ and increases in layers $m < m_0$.*

Proof. We add bars over functions and constants in the modified system to distinguish them from the original ones. The function ψ_m only depends on reaction constants and total amounts in layers $m+1, m+2, \ldots, M$. This implies that $\overline{\psi}_m$ corresponding to the modified system is equal to ψ_m for $m \geq m_0$. However, according to (14) either one of the two modifications will decrease the denominator of $\psi_{m_0-1}(y)$ and hence increase $\psi_{m_0-1}(y)$. Therefore $\overline{\psi}_{m_0-1}(y) > \psi_{m_0-1}(y)$ for all $y > 0$ in the overlap of the domains of definition of $\overline{\psi}_{m_0-1}$ and ψ_{m_0-1}, and using the recursive definition of ψ_{m-1} (14), we obtain $\overline{\psi}_m(y) > \psi_m(y)$ for all $m < m_0$. Therefore,

$$\overline{S}_{tot}^m - \overline{\lambda}_m y - \overline{\mu}_m \overline{\psi}_m(y) < S_{tot}^m - \lambda_m y - \mu_m \psi_m(y) \quad \text{for } m \leq m_0, \tag{A.1}$$

where the case $m = m_0$ follows from the assumption that either $\overline{S}_{tot}^{m_0} < S_{tot}^{m_0}$, $\overline{\mu}_{m_0} > \mu_{m_0}$, or $\overline{\lambda}_{m_0} > \lambda_{m_0}$.

Since, by definition, ξ_{m-1} (resp. $\overline{\xi}_{m-1}$) is the smallest, positive zero of the right-hand side (resp. left-hand side) of (A.1), we see that $\overline{\xi}_m < \xi_m$ for all $m < m_0$. In particular, $\overline{\rho}_M = \overline{\xi}_0 < \xi_0 = \rho_M$, and since the $\overline{\psi}_m$ are unchanged for $m \geq m_0$, we get $\overline{\rho}_m = \overline{\psi}_m(\overline{\rho}_M) = \psi_m(\overline{\rho}_M) < \psi_m(\rho_M) = \rho_m$ for $m \geq m_0$.

It remains to show that the response decreases in layers upstream from m_0, and we first consider the case $m = 1$. By the definitions of ρ_M and $\overline{\rho}_M$, we have $S_{tot}^1 - \lambda_1 \rho_M - \mu_1 \psi_1(\rho_M) = 0$ and $S_{tot}^1 - \lambda_1 \overline{\rho}_M - \mu_1 \overline{\psi}_1(\overline{\rho}_M) = 0$, so

$$\overline{\rho}_1 = \overline{\psi}_1(\overline{\rho}_M) = \frac{S_{tot}^1 - \lambda_1 \overline{\rho}_M}{\mu_1} > \frac{S_{tot}^1 - \lambda_1 \rho_M}{\mu_1} = \psi_1(\rho_M) = \rho_1.$$

Using (14) recursively, we see that

$$\psi_{m+1}(\rho_M) = \frac{S_{tot}^{m+1} - \lambda_{m+1} \rho_M}{\mu_{m+1}} - \frac{d\left(\frac{v_m}{w_n} + 1\right)\rho_M}{u_m \mu_{m+1} \psi_m(\rho_M)},$$

which for $m < m_0 - 1$ does not involve the modified parameters, and since $\psi_1(\overline{\rho}_M) > \psi_1(\rho_M)$, induction shows that

$\overline{\rho}_m = \psi_m(\overline{\rho}_M) > \psi_m(\rho_M) = \rho_m$ for all $m < m_0$, which concludes the proof. $\square$

Proposition A.2. *If λ_{m_0} or μ_{m_0} is increased, or if the total amount of substrate $S_{tot}^{m_0}$ is decreased, then the response $S_{N_m}^m$ decreases in layers $m \geq m_0$ and increases in layers $m < m_0$.*

Proof. As already argued in the proof of Proposition A.2, we have $\overline{\psi}_m = \psi_m$ (resp. $\overline{\psi}_m < \psi_m$) for $m \geq m_0$ (resp. $m < m_0$) in the overlaps of the domains of definition of the respective functions.

Let $S_{N_m}^m$ and $\overline{S}_{N_m}^m$ be the steady-state values of the response in the mth layer in each of the systems. We have $\overline{\psi}_0(\overline{S}_{N_M}^M) = c = \psi_0(S_{N_M}^M) > \overline{\psi}_0(S_{N_M}^M)$, and since $\overline{\psi}_0$ is increasing it follows that $S_{N_M}^M < \overline{S}_{N_M}^M$. Then using that ψ_m is increasing, we get $\overline{S}_{N_m}^m = \overline{\psi}_m(\overline{S}_{N_M}^M) = \psi_m(\overline{S}_{N_M}^M) > \psi_m(S_{N_M}^M) = S_{N_m}^m$ for all $m \geq m_0$. By isolating $\psi_1(y)$ in (15) and using $\overline{\psi}_0(\overline{S}_{N_M}^M) = \psi_0(S_{N_M}^M)$ and $S_{N_M}^M < \overline{S}_{N_M}^M$, we get

$$\psi_1(S_{N_M}^M) = \frac{1}{\mu_1}\left(S_{tot}^1 - \lambda_1 S_{N_M}^M - \frac{dS_{N_M}^M}{\psi_0(S_{N_M}^M)}\right)$$
$$< \frac{1}{\mu_1}\left(S_{tot}^1 - \lambda_1 \overline{S}_{N_M}^M - \frac{d\overline{S}_{N_M}^M}{\overline{\psi}_0(\overline{S}_{N_M}^M)}\right) = \overline{\psi}_1(\overline{S}_{N_M}^M),$$

and from here it follows inductively using (14) as in the proof of A.1 that $\overline{S}_{N_m}^m = \overline{\psi}_m(\overline{S}_{N_M}^M) < \psi_m(S_{N_M}^M) = S_{N_m}^m$ for all $m < m_0$. $\square$

Proposition A.3. $c_{M,\varepsilon} < c_{m,\varepsilon}$ *for all $m < M$ and $0 < \varepsilon < 1$.*

Proof. Using the definitions of $c_{M,\varepsilon}$ and $c_{m,\varepsilon}$, we obtain $c_{M,\varepsilon} = \psi_0(\varepsilon\rho_M)$ and $c_{m,\varepsilon} = \psi_0(\psi_m^{-1}(\varepsilon\psi_m(\rho_M)))$, and since both ψ_m and ψ_0^{-1} are increasing functions, $c_{M,\varepsilon} < c_{m,\varepsilon}$ if and only if $\psi_m(\varepsilon\rho_M) < \varepsilon\psi_m(\rho_M)$.

In the case $m = M$, we have $\psi_M(\varepsilon\rho_M) = \varepsilon\rho_M = \varepsilon\psi_M(\rho_M)$. Hence it suffices to prove that $\psi_m(\varepsilon\rho_M) \leq \varepsilon\psi_m(\rho_M)$ implies $\psi_{m-1}(\varepsilon\rho_M) < \varepsilon\psi_{m-1}(\rho_M)$, and this follows using $\varepsilon\rho_M < \rho_M$, since

$$\psi_{m-1}(\varepsilon\rho_M) = \frac{d\left(\frac{v_{m-1}}{w_{m-1}}+1\right)\varepsilon\rho_M}{u_{m-1}(S_{tot}^m - \lambda_m\varepsilon\rho_M - \mu_m\psi_m(\varepsilon\rho_M))}$$
$$< \varepsilon\frac{d\left(\frac{v_{m-1}}{w_{m-1}}+1\right)\rho_M}{u_{m-1}(S_{tot}^m - \lambda_m\rho_M - \mu_m\psi_m(\rho_M))} = \varepsilon\psi_{m-1}(\rho_M),$$

which finishes the proof. $\square$

Lemma A.4. *Let all reaction rates and all total amounts except S_{tot}^1 be fixed. Then $\rho_M \to \xi_1$ for $S_{tot}^1 \to \infty$ and $\rho_M \to 0$ for $S_{tot}^1 \to 0$.*

Proof. By definition, ρ_M is a root in the denominator of (15), and hence $S_{tot}^1 = \lambda_1\rho_M + \mu_1\psi_1(\rho_M)$. This function is continuous and increasing on $[0, \xi_1)$, equals 0 for $\rho_M = 0$, and tends to infinity when $\rho_M \to \xi_1^-$. The function is thus invertible, say $\rho_M = \varphi(S_{tot}^1)$, such that φ is continuous and increasing with $\varphi(0) = 0$ and satisfies $\varphi(S_{tot}^1) \to \xi_1$ for $S_{tot}^1 \to \infty$. $\square$

Lemma A.5. *For all $m < M$, the functions ψ_m and ψ_m^{-1} satisfy*

$$\psi_m'(0) = d\left(\frac{v_m}{w_m}+1\right) \bigg/ u_m S_{tot}^{m+1} \quad and$$

$$(\psi_m^{-1})'(0) = u_m S_{tot}^{m+1} \bigg/ d\left(\frac{v_m}{w_m}+1\right).$$

Proof. The first statement follows by differentiating the recursive expression for $\psi_m(y)$ (14) and inserting $y = 0$, and then the second

statement immediately follows from $(\psi_m^{-1})'(0) = 1/\psi_m'(\psi_m^{-1}(0)) = 1/\psi_m'(0)$. $\square$

Lemma A.6. *As a function of S_{tot}^1, the maximal response ρ_M satisfies*

$$\frac{d\rho_M}{dS_{tot}^1}(0) = \frac{u_1 S_{tot}^2}{\lambda_1 u_1 S_{tot}^2 + \mu_1 d\left(\frac{v_1}{w_1}+1\right)} \tag{A.2}$$

Proof. By differentiating $S_{tot}^1 = \lambda_1\rho_M + \mu_1\psi_1(\rho_M)$ with respect to S_{tot}^1, we get $\rho_M'(0) = (1 - \mu_1\psi_1'(\rho_M(0))\rho_M'(0))/\lambda_1 = (1 - \mu_1\psi_1'(0)\rho_M'(0))/\lambda_1$, and by isolating $\rho_M'(0)$ and inserting Lemma A.5, we obtain the desired result. $\square$

By plugging the expression (16) into the definition of the response coefficient (19), it follows that we have

$$\chi_{m,\varepsilon,\delta} = \underbrace{\frac{\psi_m^{-1}(\varepsilon\psi_m(\rho_M))}{\psi_m^{-1}(\delta\psi_m(\rho_M))}}_{\alpha_m}$$
$$\cdot \underbrace{\frac{S_{tot}^1 - \lambda_1\psi_m^{-1}(\delta\psi_m(\rho_M)) - \mu_1\psi_1(\psi_m^{-1}(\delta\psi_m(\rho_M)))}{S_{tot}^1 - \lambda_1\psi_m^{-1}(\varepsilon\psi_m(\rho_M)) - \mu_1\psi_1(\psi_m^{-1}(\varepsilon\psi_m(\rho_M)))}}_{\beta_m},$$

and below we will consider the factors α_m and β_m separately. $\square$

Proposition A.7. *Let all reaction rates and all total amounts except S_{tot}^1 be fixed. Then $\alpha_M = \varepsilon/\delta$, and*

$$\alpha_m \to \frac{\varepsilon}{\delta} \quad for \ S_{tot}^1 \to 0.$$

$$\alpha_m \to \begin{cases} 1 & if \ m = 1 \\ \dfrac{\psi_m^{-1}(\varepsilon\psi_m(\xi_1))}{\psi_m^{-1}(\delta\psi_m(\xi_1))} & if \ 1 < m < M \end{cases} \quad for \ S_{tot}^1 \to \infty,$$

and $\psi_m^{-1}(\varepsilon\psi_m(\xi_1))/\psi_m^{-1}(\delta\psi_m(\xi_1)) > \varepsilon/\delta$.

Proof. Since $\psi_M = \text{id}$, it immediately follows that $\alpha_M = (\varepsilon\rho_M)/(\delta\rho_M) = \varepsilon/\delta$ as claimed. According to Lemma A.4, we have $\rho \to 0$ for $S_{tot}^1 \to 0$, so since $\psi_m(0) = 0$, it follows that α_m is a 0/0–expression in the limit $S_{tot}^1 \to 0$, and we may apply L'Hôpital's rule. For the numerator of α_m (and analogously for the denominator) we have

$$\frac{d}{dS_{tot}^1}(\psi_m^{-1}(\varepsilon\rho_m)) = \frac{d\psi_m^{-1}}{dx}(\varepsilon\rho_m)\varepsilon\frac{d\rho_m}{dS_{tot}^1},$$

and using that the results of Lemma A.5 and A.6 are non-zero, it follows that

$$\frac{d}{dS_{tot}^1}(\psi_m^{-1}(\varepsilon\rho_m)) \bigg/ \frac{d}{dS_{tot}^1}(\psi_m^{-1}(\delta\rho_m)) \to \frac{\varepsilon}{\delta} \quad for \ S_{tot}^1 \to 0.$$

For the limit $S_{tot}^1 \to \infty$, we consider first the case $m = 1$. According to Lemma A.4 we have $\rho_1 = \psi_1(\rho_M) \to \infty$ for $S_{tot}^1 \to \infty$, and hence $\alpha_1 = \psi_1^{-1}(\varepsilon\rho_1)/\psi_1^{-1}(\delta\rho_1) \to \xi_1/\xi_1 = 1$, The remaining cases follow from the first part of Lemma A.4. Finally, since ψ_m is convex and increasing, the inverse ψ_m^{-1} is concave and increasing. Using $\psi_m^{-1}(0) = 0$, it follows that $\psi_m^{-1}(x)/x > \psi_m^{-1}(y)/y$ for all $x < y$. In particular, this holds for $x = \varepsilon\rho_m$ and $y = \delta\rho_m$, and hence $\psi_m^{-1}(\varepsilon\psi_m(\xi_1))/\psi_m^{-1}(\delta\psi_m(\xi_1)) > \varepsilon/\delta$. $\square$

Proposition A.8. *Let all reaction rates and all total amounts except S_{tot}^1 be fixed. Then*

$$\beta_m \to \frac{1-\delta}{1-\varepsilon} \quad for \ S_{tot}^1 \to 0$$

$$\beta_m \to \begin{cases} \dfrac{1-\delta}{1-\varepsilon} & \text{if } m = 1 \\ 1 & \text{if } 1 < m \le M \end{cases} \quad \text{for } S_{tot}^1 \to \infty.$$

Proof. To simplify notation, we denote by $f_{m,\delta}$ and $f_{m,\varepsilon}$ the numerator and denominator, respectively, of β_m. Note that β_m is a 0/0–expression in the limit $S_{tot}^1 \to 0$, and hence we may use L'Hôpital's rule. Let $z_{m,\delta} = \psi_m^{-1}(\delta\rho_m)$ such that $f_{m,\delta} = S_{tot}^1 - \lambda_1 z_{m,\delta} - \mu_1 \psi_1(z_{m,\delta})$. Then

$$\frac{df_{m,\delta}}{dS_{tot}^1} = 1 - \lambda_1 \frac{dz_{m,\delta}}{dS_{tot}^1} - \mu_1 \frac{d\psi_1}{dy}(z_m)\frac{dz_{m,\delta}}{dS_{tot}^1}$$

$$= 1 - \frac{dz_{m,\delta}}{dS_{tot}^1}\left(\lambda_1 + \mu_1\frac{d\psi_1}{dy}(z_{m,\delta})\right).$$

Now note that

$$\frac{dz_{m,\delta}}{dS_{tot}^1} = \delta\frac{d\psi_m^{-1}}{dx}(\delta\psi_m(\rho_M))\frac{d\psi_m}{dy}(\rho_M)\frac{d\rho_M}{dS_{tot}^1},$$

and by plugging in the results from Lemma A.5 and A.6, it follows that $df_{m,\delta}/dS_{tot}^1 \to 1-\delta$ for $S_{tot}^1 \to 0$. Similarly, $df_{m,\varepsilon}/dS_{tot}^1 \to 1-\varepsilon$, and hence L'Hôpital's rule implies that $\beta_m \to (1-\delta)/(1-\varepsilon)$ for $S_{tot}^1 \to 0$.

We have $f_{1,\delta} = S_{tot}^1 - \lambda_1\psi_1^{-1}(\delta\rho_1) - \mu_1\delta\rho_1$, and by combining this with $S_{tot}^1 = \lambda_1\rho_M + \mu_1\rho_1$, it follows that $f_{1,\delta} = \lambda_1(\rho_M - \psi_1^{-1}(\delta\rho_1)) + \mu_1(1-\delta)\rho_1$ and hence

$$\beta_1 = \frac{\lambda_1(\rho_M - \psi_1^{-1}(\delta\rho_1)) + \mu_1(1-\delta)\rho_1}{\lambda_1(\rho_M - \psi_1^{-1}(\varepsilon\rho_1)) + \mu_1(1-\varepsilon)\rho_1} \to \frac{1-\delta}{1-\varepsilon} \quad \text{for } S_{tot}^1 \to \infty,$$

since ρ_M and ψ_1^{-1} are bounded and $\rho_1 \to \infty$ for $S_{tot}^1 \to \infty$. For $m > 1$, we have $\psi_m(\rho_M) \to \psi_m(\xi_1)$ for $S_{tot}^1 \to \infty$, and it immediately follows that

$$\beta_m = \frac{S_{tot}^1 - \lambda_1\psi_m^{-1}(\delta\psi_m(\rho_M)) - \mu_1\psi_1(\psi_m^{-1}(\delta\psi_m(\rho_M)))}{S_{tot}^1 - \lambda_1\psi_m^{-1}(\varepsilon\psi_m(\rho_M)) - \mu_1\psi_1(\psi_m^{-1}(\varepsilon\psi_m(\rho_M)))} \to 1 \quad \text{for } S_{tot}^1 \to \infty,$$

since the last two terms in both numerator and denominator are bounded. □

By combining Propositions A.7 and A.8, we obtain Proposition 4.3 from the main text.

Appendix B. Example

Here we provide details about the calculations left out in the example in Section 4. Using the definitions of ψ_1 and ψ_2, we may write $\Delta(\varepsilon)$ on the form:

$$\Delta(\varepsilon) = \frac{r_3\varepsilon^3 + r_2\varepsilon^2 + r_1\varepsilon}{t_2\varepsilon^2 + t_1\varepsilon + t_0} = \frac{R(\varepsilon)}{T(\varepsilon)},$$

for example using computer software capable of symbolic manipulation, where the coefficients r_i and t_i only depend on the reaction constants, the total amounts, and the maximal response ρ_3. The coefficients of the polynomials may be chosen such that $t_2 < 0$ and both $T(0)$ and $T(1)$ are positive. Hence T is a second degree polynomial with negative leading coefficient, and it assumes positive values in the end points $\varepsilon = 0$ and $\varepsilon = 1$. Therefore $T(\varepsilon) > 0$ for all $0 < \varepsilon < 1$, and hence sign $\Delta(\varepsilon) = $ sign $R(\varepsilon)$.

Since $\Delta(0) = \Delta(1) = 0$, it follows that $R(0) = R(1) = 0$, and by factoring these trivial roots we obtain the last root as stated in the main text. For some constant $\tau < 0$, the polynomial $R(\varepsilon)$ factors $R(\varepsilon) = \tau \cdot \varepsilon(\varepsilon-1)(\varepsilon-\varepsilon^*) = \tau\varepsilon^3 - \tau(1+\varepsilon^*)\varepsilon^2 + \tau\varepsilon^*\varepsilon$, and hence sign $R'(0) = -\text{sign}(\varepsilon^*)$. Summing up, we know all three roots of $R(\varepsilon)$ as well as the slope of $R(\varepsilon)$ at $\varepsilon = 0$, which completely determines the sign of $R(\varepsilon)$ at any point.

Appendix C. Convergence and stability of the steady-state

We prove the convergence to a unique BMSS of the phosphorelay for any set of positive initial conditions using Theorem 2 in Angeli et al. (2010). We will restate the theorem here, but first we introduce some concepts from Angeli et al. (2010). To simplify notation, we use $\leftrightarrow$ to denote reversible reactions in inline text.

For a reaction $A \to B$, A is the *reactant* and B is the *product*, and for every reversible reaction e.g. $S_n^m \leftrightarrow S_{n+1}^m$, a direction is chosen so that the reactant and the product are well-defined. For the reversible reactions in (1)–(3), we choose the left-hand side to be the reactant and the right-hand side to be the product. We have a total of $n_S = \sum_{m=1}^{M} N_m + M - 1$ species and $n_R = \sum_{m=1}^{M} N_m + M$ reactions in the system. Define the $n_S \times n_R$ *stoichiometric matrix* Γ such that the entry $\Gamma_{s,r}$ corresponding to species s and reaction r is 1 if s is in the reactant of r, -1 if s is in product, and zero otherwise. Here orders on the sets of species and reactions are implicitly chosen.

The *directed SR-graph* is constructed as follows: The set of vertices is the union of the set of species (called *species nodes*) and the set of reactions (called *reaction nodes*). If a species s takes part in a reversible reaction r or is part of the reactant of an irreversible reaction r, there are edges $s \to r$ and $r \to s$. If s is part of the product of an irreversible reaction r, there is an edge $r \to s$. A *siphon* Σ is a non-empty subset of species such that if $s \in \Sigma$ is in the product of a reaction r, then Σ contains at least one species in the reactant of r. Here reversible reactions are considered as two different irreversible reactions, so that each side of the reversible reaction appears as product in one reaction and as reactant in the other. A siphon is *minimal* if it contains no siphon other than itself.

Theorem 2 in Angeli et al. (2010) states that all solutions of the phosphorelay ODEs in $\mathbf{R}_{>0}^{n_S}$ converge to a unique equilibrium if the following four conditions hold:

(i) The system of ODEs of the phosphorelay is persistent.
(ii) For all species s and reactions $r_1 \ne r_2$, the product $-\Gamma_{s,r_1}\Gamma_{s,r_2}$ is non-negative.
(iii) There is a directed path between any two reaction nodes in the directed SR-graph.
(iv) The kernel of Γ contains a positive vector.

Remark. With the notions from Angeli et al. (2010), conditions (ii) and (iii) imply that the corresponding system in reaction coordinates is monotone with respect to the positive orthant cone, and strongly monotone in the interior with respect to that order. This is a consequence of Proposition 5.3 and the proof of Theorem 1 in Angeli et al. (2010).

We will now prove (i)–(iv). By the choice of directions of reactions in our system, each species is on the left of exactly one reaction and on the right of exactly one reaction. It follows that for each species s there are exactly two reactions r_1, r_2 such that $\Gamma_{s,r_1}, \Gamma_{s,r_2} \ne 0$ and further that they have opposite sign. Thus, $\Gamma_{s,r_1}\Gamma_{s,r_2} < 0$ and zero for all other choices of reactions. This proves (ii). Each row of Γ has only two non-zero entries, and they are of opposite signs. Therefore the vector $(1, \ldots, 1)$ belongs to the kernel of Γ, and hence (iv) holds.

To show (iii), note that for a fixed m, there is a path in the directed SR-graph between any two reaction nodes of the form:
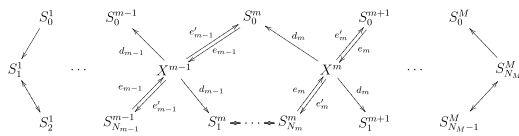
$$r_{n,m}: S_n^m \leftrightarrow S_{n+1}^m, \quad e_m: S_{N_m}^m + S_0^{m+1} \leftrightarrow X^m, \quad \text{or} \quad d_m: X^m \to S_0^m + S_1^{m+1}.$$

For $m = M$ the statement is true with the last two reactions replaced by $d_0: S_{N_M}^M \to S_0^M$. Furthermore, there is a path from w_m to $r_{1,m+1}$ and to e_{m-1}, connecting reactions in different layers.

There is a path from the reaction node $e_0\colon S_0^1 \to S_1^1$ to $r_{1,1}$ and from d_1 to e_0. Therefore, a directed path between any two reactions of the phosphorelay exists, and (iii) holds.

All that is left is to prove (i). For that, we use Theorem 2 in Angeli et al. (2007) that states that if (a) the network has a positive conservation law and (b) there is a conservation law with non-negative coefficients on the species for each minimal siphon, then the network is persistent. Since each species of the phosphorelay is part of a conservation law with non-negative coefficients (5), it follows that (a) holds.

If we show that the sets $\Sigma_m = \{S_0^m, S_1^m, \ldots, S_{N_m}^m, X^{m-1}, X^m\}$ for $m = 1, 2, \ldots, M$ (removing the non-defined X^0, X^M for $m = 1, M$) are the minimal siphons, then the conservation law (5) ensures that (b) holds and the proof is completed. We construct a graph that gives an easy visual inspection of which the minimal siphons of the phosphorelay are. If r is a reaction that contains a species s_1 in the reactant and a species s_2 in the product, then we draw an edge $s_1 \overset{r}{\to} s_2$ with label r. The graph is

where d_m is as above, $e_m\colon S_{N_m}^m + S_0^{m+1} \to X^m$, and $e_m'\colon X^m \to S_{N_m}^m + S_0^{m+1}$. The labels of the reactions $r_{n,m}\colon S_n^m \leftrightarrow S_{n+1}^m$ are not shown.

Let Σ be a siphon. Then inspection of the graph gives:

(1) If S_n^m belongs to Σ for some $n > 0$, then so do $S_{n'}^m$ for all $n' > 0$.
(2) If S_n^m belongs to Σ for some $n \geq 0$, then so do X^m and X^{m-1}. Further, if S_n^1 or S_0^M belong to Σ then so do S_0^1 and $S_{N_M}^M$, respectively.
(3) If X^m belongs to Σ, then either S_0^{m+1} or $S_{N_m}^m$ (and thus S_n^m for all $n > 0$) belong to Σ.

It is easy to see that the middle pentagon which contains the species in Σ_m is a siphon for all $1 \leq m \leq M$, and conditions (1)–(3) ensure that it is minimal. If Σ is a siphon that does not contain Σ_m for any m, then (1)–(3) imply that it must contain X^m for all m. If S_0^m does not belong to Σ for any m, then by (3) S_n^m belongs to Σ for all m and $n > 0$. It follows from (2) that so does S_0^1 and $\Sigma_1 \subseteq \Sigma$, thereby reaching a contradiction. Thus, there is an m for which S_0^m belongs to Σ. Since $S_{N_m}^m$ does not ($\Sigma_m \nsubseteq \Sigma$), by (3) S_0^{m+1} belongs to Σ. We repeat the argument to conclude that $S_0^M \in \Sigma$. It follows from (2) that so does $S_{N_M}^M$ and $\Sigma_M \subseteq \Sigma$, again reaching a contradiction. Therefore, any siphon contains Σ_m for some m as desired.

References

Angeli, D., de Leenheer, P., Sontag, E.D., 2007. A Petri net approach to the study of persistence in chemical reaction networks. Math. Biosci. 210 (2), 598–618.

Angeli, D., de Leenheer, P., Sontag, E., 2010. Graph-theoretic characterizations of monotonicity of chemical networks in reaction coordinates. J. Math. Biol. 61 (4), 581–616.

Appleby, J., Parkinson, J., 1996. Signal transduction via the multi-step phosphorelay: not necessarily a road less traveled. Cell 86, 845–848.

Banaji, M., Craciun, G., 2010. Graph-theoretic criteria for injectivity and unique equilibria in general chemical reaction systems. Adv. Appl. Math. 44 (2), 168–184.

Barkai, N., Leibler, S., 1997. Robustness in simple biochemical networks. Nature 387 (6636), 913–917.

Batchelor, E., Goulian, M., 2003. Robustness and the cycle of phosphorylation and dephosphorylation in a two-component regulatory system. Proc. Natl. Acad. Sci. USA 100 (2), 691–696.

Blüthgen, N., Bruggeman, F.J., Legewie, S., Herzel, H., Westerhoff, H.V., Kholodenko, B.N., 2006. Effects of sequestration on signal transduction cascades. FEBS J. 273 (5), 895–906.

Burbulys, D., Trach, K.A., Hoch, J.A., 1991. Initiation of sporulation in B. subtilis is controlled by a multicomponent phosphorelay. Cell 64 (3), 545–552.

Chang, C., Stewart, R.C., 1998. The two-component system. Regulation of diverse signaling pathways in prokaryotes and eukaryotes. Plant Physiol. 117 (3), 723–731.

Cohen, P., 2000. The regulation of protein function by multisite phosphorylation-a 25 year update. Trends Biochem. Sci. 25 (12), 596–601.

Conradi, C., Flockerzi, D., Raisch, J., 2008. Multistationarity in the activation of a MAPK: parametrizing the relevant region in parameter space. Math. Biosci. 211 (1), 105–131.

Cotter, P.A., Jones, A.M., 2003. Phosphorelay control of virulence gene expression in Bordetella. Trends Microbiol 11 (8), 367–373.

Csikász-Nagy, A., Cardelli, L., Soyer, O.S., 2011. Response dynamics of phosphorelays suggest their potential utility in cell signalling. J. Roy. Soc. Interface 8 (57), 480–488.

Feliu, E., Wiuf, C., 2011. Variable elimination in chemical reaction networks with mass action kinetics. arXiv:1109.1505v1.

Feliu, E., Wiuf, C., Enzyme sharing as a cause of multistationarity in signaling systems. J. Roy. Soc. Interface, doi:10.1098/rsif.2011.0664, in press.

Feliu, E., Knudsen, M., Andersen, L.N., Wiuf, C., 2012a. An algebraic approach to signaling cascades with n layers. Bull. Math. Biol. 74, 45–72.

Feliu, E., Knudsen, M., Wiuf, C., 2012b. Signaling cascades: consequences of varying substrate and phosphatase levels. Adv. Exp. Med. Biol. 736 (1), 81–94.

Fujita, M., Losick, R., 2005. Evidence that entry into sporulation in Bacillus subtilis is governed by a gradual increase in the level and activity of the master regulator Spo0A. Genes Dev. 19 (18), 2236–2244.

Goldbeter, A., Koshland, D.E., 1981. An amplified sensitivity arising from covalent modification in biological systems. Proc. Natl. Acad. Sci. USA 78 (11), 6840–6844.

Goldbeter, A., Koshland, D.E., 1984. Ultrasensitivity in biochemical systems controlled by covalent modification. Interplay between zero-order and multi-step effects. J. Biol. Chem. 259 (23), 14441–14447.

Gunawardena, J., 2005. Multisite protein phosphorylation makes a good threshold but can be a poor switch. Proc. Natl. Acad. Sci. USA 102 (41), 14617–14622.

Gunawardena, J., 2007. Distributivity and processivity in multisite phosphorylation can be distinguished through steady-state invariants. Biophys. J. 93 (11), 3828–3834.

Gunawardena, J., 2010. Biological systems theory. Science 328 (5978), 581–582.

Hoch, J.A., 1993. Regulation of the phosphorelay and the initiation of sporulation in Bacillus subtilis. Ann. Rev. Microbiol. 47, 441–465.

Huang, C.Y., Ferrell, J.E., 1996. Ultrasensitivity in the mitogen-activated protein kinase cascade. Proc. Natl. Acad. Sci. USA 93 (19), 10078–10083.

Kapuy, O., Barik, D., Sananes, M.R.D., Tyson, J.J., Novák, B., 2009. Bistability by multiple phosphorylation of regulatory proteins. Prog. Biophys. Mol. Biol. 100 (1–3), 47–56.

Kim, J.-R., Cho, K.-H., 2006. The multi-step phosphorelay mechanism of unorthodox two-component systems in E. coli realizes ultrasensitivity to stimuli while maintaining robustness to noises. Comput. Biol. Chem. 30 (6), 438–444.

Li, F., Long, T., Lu, Y., Ouyang, Q., Tang, C., 2004. The yeast cell-cycle network is robustly designed. Proc. Natl. Acad. Sci. USA 101 (14), 4781–4786.

Maeda, T., Wurgler-Murphy, S.M., Saito, H., 1994. A two-component system that regulates an osmosensing MAP kinase cascade in yeast. Nature 369 (6477), 242–245.

Manrai, A.K., Gunawardena, J., 2008. The geometry of multisite phosphorylation. Biophys. J. 95 (12), 5533–5543.

Markevich, N.I., Hoek, J.B., Kholodenko, B.N., 2004. Signaling switches and bistability arising from multisite phosphorylation in protein kinase cascades. J. Cell Biol. 164 (3), 353–359.

Mizuno, T., 1997. Compilation of all genes encoding two-component phosphotransfer signal transducers in the genome of Escherichia coli. DNA Res. 4, 161–168.

Molle, V., Fujita, M., Jensen, S.T., Eichenberger, P., González-Pastor, J.E., Liu, J.S., Losick, R., 2003. The Spo0A regulon of Bacillus subtilis. Mol. Microbiol. 50 (5), 1683–1701.

Ohlsen, K.L., Grimsley, J.K., Hoch, J.A., 1994. Deactivation of the sporulation transcription factor Spo0A by the Spo0E protein phosphatase. Proc. Natl. Acad. Sci. USA 91 (5), 1756–1760.

Perego, M., Hoch, J.A., 1996. Protein aspartate phosphatases control the output of two-component signal transduction systems. Trends Genet. 12 (3), 97–101.

Perraud, A.L., Weiss, V., Gross, R., 1999. Signalling pathways in two-component phosphorelay systems. Trends Microbiol. 7 (3), 115–120.

Posas, F., Wurgler-Murphy, S.M., Maeda, T., Witten, E.A., Thai, T.C., Saito, H., 1996. Yeast HOG1 MAP kinase cascade is regulated by a multistep phosphorelay mechanism in the SLN1-YPD1-SSK1 "two-component" osmosensor. Cell 86 (6), 865–875.

Russo, F., Silhavy, T., 1991. EnvZ controls the concentration of phosphorylated OmpR to mediate osmoregulation of the porin genes. J. Mol. Biol. 222, 567–580.

Saito, H., 2001. Histidine phosphorylation and two-component signaling in eukaryotic cells. Chem. Rev. 101 (8), 2497–2509.

Salazar, C., 2009. Multisite protein phosphorylation-from molecular mechanisms to kinetic models. FEBS J. 276, 3177–3198.

Salazar, C., Höfer, T., 2007. Versatile regulation of multisite protein phosphorylation by the order of phosphate processing and protein–protein interactions. FEBS J. 274 (4), 1046–1061.

Shinar, G., Feinberg, M., 2010. Structural sources of robustness in biochemical reaction networks. Science 327 (5971), 1389–1391.

Shinar, G., Milo, R., Martínez, M.R., Alon, U., 2007. Input–output robustness in simple bacterial signaling systems. Proc. Natl. Acad. Sci. USA 104 (50), 19931–19935.

Stock, A.M., Robinson, V.L., Goudreau, P.N., 2000. Two-component signal transduction. Ann. Rev. Biochem. 69, 183–215.

Thomson, M., Gunawardena, J., 2009a. Unlimited multistability in multisite phosphorylation systems. Nature 460 (7252), 274–277.

Thomson, M., Gunawardena, J., 2009b. The rational parameterisation theorem for multisite post-translational modification systems. J. Theor. Biol. 261 (4), 626–636.

Uhl, M., Miller, J., 1996. Integration of multiple domains in a two-component sensor protein: the *Bordetella pertussis* BvgAS phosphorelay. EMBO J. 15 (5), 1028–1036.

Ventura, A.C., Sepulchre, J.-A., Merajver, S.D., 2008. A hidden feedback in signaling cascades is revealed. PLoS Comput. Biol. 4 (3), e1000041.

Wang, L., Sontag, E.D., 2007. On the number of steady states in a multiple futile cycle. J. Math. Biol. 57 (1), 29–52.

West, A.H., Stock, A.M., 2001. Histidine kinases and response regulator proteins in two-component signaling systems. Trends Biochem. Sci. 26 (6), 369–376.

Zhang, W., Shi, L., 2005. Distribution and evolution of multiple-step phosphorelay in prokaryotes: lateral domain recruitment involved in the formation of hybrid-type histidine kinases. Microbiology 151, 2159–2173.